Adsorption and Aggregation of *meso*-Tetrakis(4-carboxyphenyl)porphyrinato Zinc(II) at the Polarized Water|1,2-Dichloroethane Interface

Hirohisa Nagatani,[†,‡] Zdeněk Samec,[§] Pierre-François Brevet,[||] David J. Fermín,[†] and Hubert H. Girault*[,†]

Laboratoire d'Electrochimie Physique et Analytique, Institut de Chimie Moléculaire et Biologique, Ecole Polytechnique Fédérale de Lausanne, CH-1015 Lausanne, Switzerland, J. Heyrovský Institute of Physical Chemistry, Academy of Science of the Czech Republic, Dolejškova 3, CR-18223 Prague 8, Czech Republic, and Laboratoire de Spectrométrie Ionique et Moléculaire, Université Claude Bernard Lyon 1, UMR, CNRS 5579, F-69622 Villeurbanne Cedex, France

Received: August 22, 2002

The specific adsorption of the water-soluble *meso*-tetrakis(4-carboxyphenyl)porphyrinato zinc(II) ($ZnTPPC^{4-}$) was studied at the polarizable water|1,2-dichloroethane (DCE) interface by surface second harmonic (SH) generation and quasi-elastic laser scattering (QELS). The intense SH responses were analyzed as a function of the $ZnTPPC^{4-}$ concentration and of the Galvani potential difference. It was confirmed that the coverage of ZnTPPC increases as the Galvani potential difference approaches the formal ion transfer potential. In this potential range, the high interfacial concentration induces the formation of *J*-aggregates at the interface. The aggregation phenomena manifest itself by a red-shift of the SH response resonant to the Soret band and an overall increase in the SH intensity. At potentials more positive than the formal transfer potential, the SH spectrum exhibits a maximum at the same wavelength of absorption of ZnTPPC in solution, suggesting a low extent of aggregation in the porphyrin assembly. The ZnTPPC adsorption also manifests itself by changes in the frequency of the microscopic thermal fluctuation (capillary waves) at the liquid|liquid boundary. The potential dependence of the capillary waves frequency was estimated from QELS, allowing the construction of electrocapillary curves at various ZnTPPC concentrations.

1. Introduction

Porphyrin derivatives exhibit unique interfacial properties relevant to a variety of process involved in oxygen transport in vivo, molecular recognition, photodynamic therapy, enzymatic reactions, oxygen reduction, as well as molecular photovoltaic and luminescent devices.[1,2] In particular, the zinc(II) porphyrins show significantly high photoreactivity[3] and the self-assembly of these molecules yields supramolecular organization.[4,5] Recently, the adsorption reactions of zinc(II) porphyrins have been studied at polarizable and nonpolarizable liquid|liquid interfaces by a variety of spectroscopic techniques.[6−10] Kinetic studies of processes such as demetalation and protonation have shown that the rate-determining step of the interfacial reaction is significantly different from the homogeneous reaction mechanism.[7] Water-soluble zinc(II) porphyrin has been studied as a sensitizer for photoinduced electron-transfer reactions at polarizable liquid|liquid interfaces.[11−15] Under potentiostatic conditions, the heterogeneous photoinduced electron transfer involving specifically adsorbed porphyrins and redox couples in the organic phase manifests itself as photocurrent responses. In the case of the anionic *meso*-tetrakis(4-carboxyphenyl)porphyrinato zinc(II) (ZnTPPC) and lipophilic ferrocene derivatives at the water|1,2-dichloroethane (DCE) interface, the photocurrent efficiency is determined not only by the quantum yield but also by the coverage of the specifically adsorbed ZnTPPC.[11,16] In addition to the interfacial coverage, photocurrent anisotropy under linearly polarized light provided information on the average molecular orientation of the photoactive species.[13,17] For instance, it was observed that ZnTPPC adopts a rather coplanar position with respect to the liquid|liquid boundary in the low coverage region.[13] A number of issues remain to be addressed in this system, e.g., the role of oxygen, interfacial protonation, and intermolecular interactions, which requires a detailed analysis of the electronic structure of the adsorbed species. These issues are not only relevant to light energy conversion purposes but also for designing efficient dyes for photodynamic therapy of cancer cells.

Nonlinear optics is one of the most powerful approaches available for the electronic characterization of adsorbed species at molecular interfaces.[18,19] Recent surface second harmonic (SH) generation investigation of the *meso*-tetrakis(*N*-methyl-4-pyridyl)porphyrin (H_2TMPyP^{4+}) and its zinc(II) complex ($ZnTMPyP^{4+}$) at the water|DCE interface demonstrated that a large second harmonic (SH) signal was generated upon specific adsorption.[20] The coverage of both species appeared dependent on the Galvani potential difference, whereas evidence was obtained of the formation of the *J* aggregate of ZnTMPyP at the liquid|liquid boundary.[20]

In the present work, the adsorption behavior of ZnTPPC was examined at the water|DCE interface under potentiostatic control. The dependence of the SH responses on the applied potential confirmed that the surface coverage of ZnTPPC increases as the Galvani potential difference approaches the

* To whom correspondence should be addressed. Fax: +41-21-693-3667. E-mail: Hubert.Girault@epfl.ch.
† Ecole Polytechnique Fédérale de Lausanne.
‡ Present address: Department of Natural Sciences, Hyogo University of Teacher Education, Yashiro, Hyogo 673-1494, Japan.
§ Academy of Science of the Czech Republic.
|| Université Claude Bernard Lyon 1.

10.1021/jp026819b CCC: $25.00
Published on Web 12/18/2002

Ag	Ag_2SO_4	ZnTPPC 1×10^{-2} mol dm^{-3} Li_2SO_4 (aq)	5×10^{-3} mol dm^{-3} BTPPATPBCl (DCE)	1×10^{-3} mol dm^{-3} BTPPACl 1×10^{-2} mol dm^{-3} LiCl (aq)	AgCl	Ag

Figure 1. Composition of electrochemical cell.

formal ion transfer potential. Furthermore, the formation of *J* aggregates takes place at high ZnTPPC coverage. The adsorption behavior of ZnTPPC was also monitored by quasi-elastic laser scattering (QELS).

2. Experimental Section

2.1. Reagents. The water-soluble anionic porphyrin, *meso*-tetrakis(4-carboxyphenyl)porphyrinato zinc(II) tetrasodium salt ($Na_4ZnTPPC$) was purchased from Porphyrin Products and used without further purification. The hydrophobic organic salts of porphyrin, $(ZnTPPC^{4-})(BTPPA^+)_4$, was prepared by metathesis of $Na_4ZnTPPC$ with bis(triphenylphosphoranylidene)ammonium chloride (BTPPACl) in a 2:1 mixture of methanol and water.

The electrolytes for the aqueous and the organic phases were 1.0×10^{-2} mol dm^{-3} lithium sulfate and 5×10^{-3} mol dm^{-3} bis(triphenylphosphoranylidene)ammonium tetrakis(4-chlorophenyl)borate (BTPPATPBCl), respectively. The electrochemical cell is schematically shown in Figure 1. The Galvani potential difference ($\Delta_o^w\phi$) was calculated by taking a value of 0.160 V for the formal ion transfer potential ($\Delta_o^w\phi'_{TMA^+}$) of the tetramethylammonium cation (TMA^+). The aqueous and the organic solutions were prepared with purified water from a Milli-Q system (Millipore Milli-Q.185) and 1,2-dichloroethane (DCE) (Fluka 98% for HPLC), respectively. All other reagents used were of analytical grade.

2.2. SSHG Measurements. The fundamental beam at frequency ω was provided by an optical parametric oscillator (OPO) (Spectra-Physics MOPO-710) pumped with the third harmonic of a Q-switched Nd^{3+}:YAG laser (Spectra-Physics Quanta-Ray GCR-170−10 220 mJ at 10 Hz). The fundamental wavelength was tuned from 780 to 1020 nm. The fundamental beam was reflected at the water|DCE interface under the TIR condition with the angle of incidence of ca. 70°. The energy of a laser pulse provided to the interface was typically 2.8 mJ at 900 nm. The second harmonic (SH) signal at the frequency 2ω generated at the interface was detected by a photomultiplier tube through a monochromator (Jobin-Yvon SPEX 270-M) after passing through band-pass filters to cut the fundamental beam. To take into account the wavelength dependence of the fundamental beam energy, ca. 2% of the output from the OPO was split by a beam splitter toward a laser power meter (Ophir Optronics PE-10) and the collected SH signal was normalized by dividing the SH intensity by the square of the laser energy. The fundamental beam was *p*-polarized unless otherwise noted. The water|DCE interface formed in a rectangular optical quartz cell with an area of 4.0×2.0 cm^2 was electrochemically polarized by a custom-made four-electrode potentiostat with a waveform generator (Hi-Tek Instruments PP-R1). Platinum wires were used as counter-electrodes in both phases. The absorption spectra of the bulk phases were measured by a UV−visible spectrophotometer (Varian Cray 1E).

2.3. Interfacial Tension Measurements. The electrocapillary curves were obtained from QELS measurements as a function of the Galvani potential difference.[21−24] A schematic drawing of the experimental set up is displayed in Figure 2. The optical cell was a cylindrical glass cell with an interfacial area of 15.9 cm^2, and the water surface was covered with the optical glass

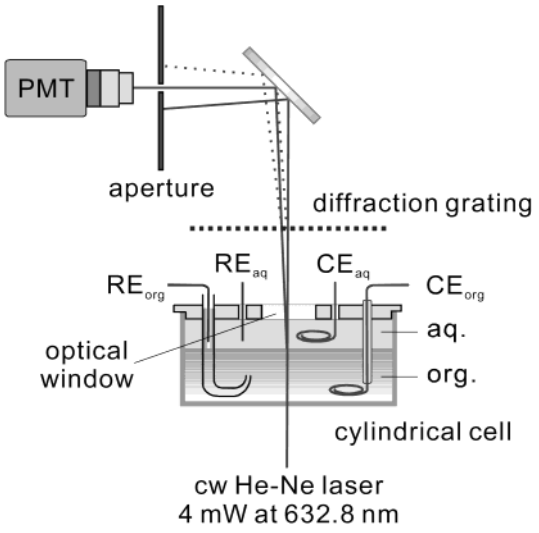

Figure 2. Schematic drawing of the experimental set up of QELS.

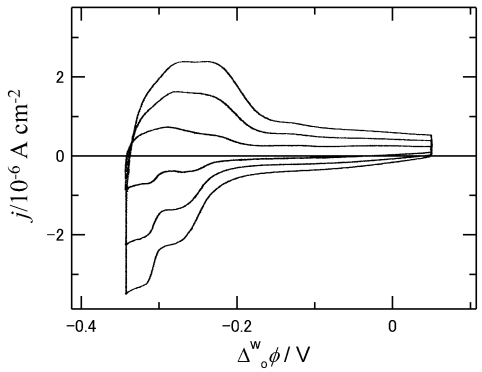

Figure 3. Cyclic voltammograms measured for ZnTPPC at 5, 10, and 25 mV s^{-1}. The concentration of ZnTPPC in the aqueous phase was 2.0×10^{-5} mol dm^{-3}.

window to minimize light scattering from the water|air interface. The Galvani potential difference was controlled by a four-electrode potentiostat under identical conditions as for the SSHG measurements (Figure 1). The aqueous and the organic phases were saturated with each other. The laser light beam passing through the interface perpendicularly was a cw He−Ne laser of 4 mW at 632.8 nm (Uniphase model 1101). The diffraction grating consisting of dark lines with 0.285 mm spacing prepared on a photographic glass plate was placed after the optical cell. The grating constant (*d*) was determined as 0.335 mm by following equation:[23]

$$n\lambda = d \sin \alpha \qquad (1)$$

where *n* is the order of the diffraction spot, λ is the wavelength of the incident light, and α is the angle of the diffracted beam with respect to the fundamental beam at the detector plane, i.e., 1.08° for the tenth order spot. The optical beat of third-order diffraction spot was monitored by a photomultiplier tube and was analyzed by a fast-Fourier transform (FFT) analyzer (Stanford Research Systems SR770). All of the experiments were carried out in a thermostated room at 295 ± 2 K.

3. Results and Discussion

3.1. Potential Induced Adsorption of ZnTPPC. Cyclic voltammograms measured in the presence of 2.0×10^{-5} mol dm^{-3} ZnTPPC in the aqueous phase are shown in Figure 3.

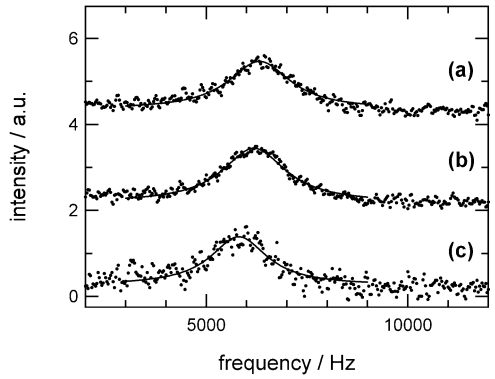

Figure 4. Typical power spectra of third-order diffracted spot from the polarized water|DCE interface. The solid lines were obtained by a least-squares curve fitting using a Lorentzian function. The applied potential was −0.20 V. The concentration of ZnTPPC in the aqueous phase was 0 (a), 5×10^{-6} mol dm^{-3} (b), and 5×10^{-5} mol dm^{-3} (c).

ZnTPPC exhibited rather complex voltammetric responses such as the broad ion transferring peak with pre- and post-transfer responses associated with adsorption processes at the interface. These responses are substantially different to those observed in the presence of *meso*-tetrakis(4-sulfonatophenyl)porphyrinato zinc (II) ($ZnTPPS^{4-}$) under identical conditions.[10,12] The transfer of $ZnTPPS^{4-}$ across the water|DCE interface exhibits a sharp voltammetric signal with a peak-to-peak separation of 15 mV. Although the overlapping of the ion transfer with the adsorption response close to the potential window edge introduces difficulties for the analysis, the formal ion transfer potential of ZnTPPC ($\Delta_o^w\phi^{o\prime}_{ZnTPPC}$) was estimated to be ca. −0.25 V.

The specific adsorption of ZnTPPC at potentials close to $\Delta_o^w\phi^{o\prime}_{ZnTPPC}$ is expected to manifest itself by significant changes in the interfacial tension. The dependence of the power spectrum for the optical beat of third-order diffracted beam from QELS on the ZnTPPC concentration at −0.20 V is illustrated in Figure 4. The frequency of maximum intensity (f_0), associated with the mean frequency of the capillary waves, was determined by a least-squares curve fitting employing a Lorentzian function. It is observed that the characteristic frequency f_0 decreases with increasing concentration of ZnTPPC, indicating a decrease in the interfacial tension. The relation between the interfacial tension (γ_i) and f_0 is given by the Lamb's equation:[25]

$$f_0 = \frac{1}{2\pi}\sqrt{\frac{\gamma_i k^3}{\rho^w + \rho^{org}}} \qquad (2)$$

where k is the capillary wavenumber and ρ^w and ρ^{org} are the density of water (0.9978 g cm^{-3}) and DCE (1.240 g cm^{-3}), respectively. For the configuration employed in all measurements, the effective value of $k = 512.7$ cm^{-1} was experimentally estimated by taking the interfacial tension of the neat water|DCE interface as 28.5 m N m^{-1}.[26] The electrocapillary curves displayed in Figure 5 shows that γ_i decreases at negative potentials in the presence of 5.0×10^{-6} mol dm^{-3} ZnTPPC in comparison to the values obtained for the water|DCE interface in the absence of the porphyrin. The effect of ZnTPPC adsorption on the interfacial tension was extended to 0.20 V for a ZnTPPC concentration of 5.0×10^{-5} mol dm^{-3}. Although the rather negative formal ion transfer potential indicates a high hydrophilicity of ZnTPPC, these results show that the adsorption takes place at potentials substantially more positive than $\Delta_o^w\phi^{o\prime}_{ZnTPPC}$. The surface excess of ZnTPPC (Γ_i) can be

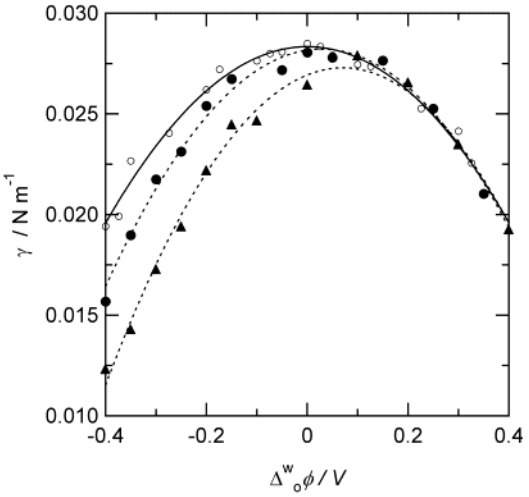

Figure 5. Electrocapillary curves measured by QELS. The concentration of ZnTPPC in the aqueous phase was 0 (circle), 5.0×10^{-6} mol dm^{-3} (square), and 5.0×10^{-5} mol dm^{-3} (triangle).

evaluated by the Gibbs surface tension equation:

$$\Gamma_i = -\frac{1}{RT}\frac{d\gamma_i}{d\ln c^w} \qquad (3)$$

where c^w is the concentration of ZnTPPC in the aqueous phase. From eq 3, the values of the surface excess at 0 V in the presence of 5.0×10^{-6} mol dm^{-3} and 5.0×10^{-5} mol dm^{-3} ZnTPPC corresponds to 3×10^{-12} mol cm^{-2} and ca. 2.8×10^{-11} mol cm^{-2} respectively. Assuming the formation of a monolayer, the surface coverage is evaluated as 0.05 for 5.0×10^{-6} mol dm^{-3} and 0.38 for 5.0×10^{-5} mol dm^{-3} ZnTPPC, taking the interfacial area for one porphyrin molecule as 2.3 nm^2 as estimated by molecular mechanics (MM2) calculations. At more negative potentials, the interfacial tension exhibits a stronger dependence on the ZnTPPC concentration, indicating a larger value of the surface coverage. For instance, the coverage at −0.4 V can be estimated as 0.80 for a concentration of 5.0×10^{-5} mol dm^{-3}. Although the potential dependence of the ZnTPPC adsorption as revealed by QELS is entirely compatible to the results previously obtained by photoelectrochemical measurements,[11,13,16] the latter provide somewhat larger values for the coverage at more positive potentials. However, as discussed below, a quantitative analysis of the ZnTPPC organization at the liquid|liquid boundary is rather complex because of the contribution of a variety of phenomena such as partial protonation of the peripheral carboxyphenyl groups and cooperative hydrogen bonding,[13] as well as aggregation phenomena.

3.2. Surface SH Spectrum of ZnTPPC at the Neat Water|DCE Interface. Surface SH spectra of ZnTPPC at the neat water|DCE interface obtained at two different concentrations are contrasted to the absorption spectrum of the porphyrin in aqueous solution in Figure 6. Two interesting aspects can be highlighted from these results: the relative high intensity of the SH signal and the bathochromic shift of the SH maximum with respect to the Soret band. Considering that the second order polarizability of symmetrically substituted porphyrins is rather small,[27,28] the SH responses in Figure 6 may involve a substantial contribution from optical transitions associated with excitonic levels in strongly interacting adsorbed porphyrins or aggregates. In this case, the SH responses cannot be solely described in terms of the so-called dipole approximation that describes the macroscopic second-order susceptibility in terms of the microscopic second-order polarizability.

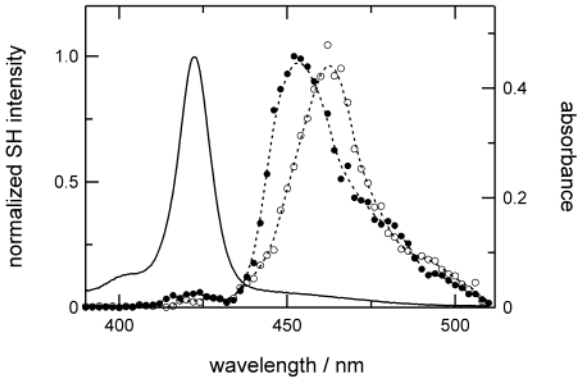

Figure 6. Surface SH spectra of ZnTPPC at the water|DCE interface. The concentration of ZnTPPC in the aqueous phase was 5.0×10^{-5} mol dm^{-3} (hollow circle) and 2.0×10^{-4} mol dm^{-3} (filled circle). The solid line is the absorption spectrum of ZnTPPC in the aqueous solution.

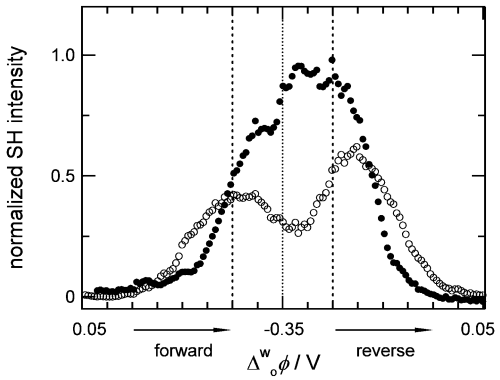

Figure 7. Potential dependence of SH intensities at 420 nm (hollow circles) and 460 nm (filled circles). The concentration of ZnTPPC in the aqueous phase was 5.0×10^{-6} mol dm^{-3}. The dashed lines indicate the formal ion transfer potential of ZnTPPC at -0.25 V.

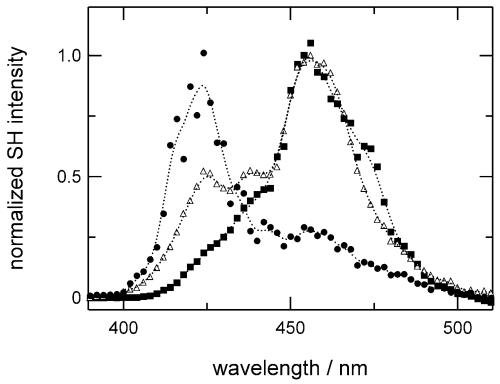

Figure 8. Potential dependence of surface SH spectrum. The applied potential was kept at -0.15 (filled circles), -0.20 (hollow triangles), and -0.25 V (filled squares), respectively. The concentration of ZnTPPC in the aqueous phase was 5.0×10^{-6} mol dm^{-3}.

As shown in Figure 6, the maximum of the SH spectrum for a concentration of 5×10^{-5} mol dm^{-3} is located at 454 nm. Upon increasing concentration of ZnTPPC, the maximum signal further shifts to wavelengths around 460 nm. Considering that the Soret band for ZnTPPC in the aqueous and DCE phases is centered at 422.5 and 423.5 nm respectively, it can be concluded that these SH responses are in resonance with excitonic transitions associated with the porphyrin aggregates. Khairutdinov and Serpone have reported broad multicomponent optical transition from aggregates of the free base H_2TPPC centered at 392, 425, 442, and 460 nm.[29] The homogeneous aggregation of H_2TPPC takes place at pH = 3.5, in which electrostatic repulsion is minimized by protonation of the peripheral carboxylic groups. The results shown in Figure 6 suggest that protonation of the carboxyphenyl groups occurs at the interfacial boundary even at pH close to 7 in the aqueous phase. Indeed, previous studies have also shown that the coverage of ZnTPPC at the water|DCE interface and the corresponding excess charge strongly decreases upon increasing the pH from 7 to 10,[13] indicating that the adsorbed species involved partially protonated forms of the porphyrin.

Weak SH responses are also observed at 423 nm, i.e., in resonance with the Soret band of the nonaggregated form of ZnTPPC. The difference in the relative intensity between the aggregated and nonaggregated form revealed the enhancement of the nonlinear optical responses because of the presence of excitonic levels. Mukamel and co-workers have studied the dependence of the third-order susceptibility $\chi^{(3)}$ on the size of molecular aggregates featuring Frenkel-type excitons.[30−32] These works show that for *N*-interacting particles with homogeneously broadened two-level transitions, the enhanced transition dipole moment can combine to produce a N^2 dependence of $\chi^{(3)}$. However, Knoester has argued that the collective enhancement can be damped by disordering in the aggregate structure.[33] Although a detailed analysis of the SH responses arising from the porphyrin aggregates is beyond the scope of this publication, the experimental evidence appear to show that a major contribution to the nonlinear responses arises from $\chi^{(3)}$. We shall come back to this point at the end of the discussion.

3.3. Potential Dependence of the Adsorption and Aggregation of ZnTPPC. The SH responses in the presence of ZnTPPC were analyzed as a function of the Galvani potential difference. As illustrated by the electrocapillary curves shown in Figure 5, the excess concentration of ZnTPPC decreases as $\Delta^{w}_{o}\phi$ is increased. Previous studies have shown that the coverage of ionic species is dependent on the fraction of the applied potential acting on the adsorption plane as well as the stabilization energy associated with the adsorbed layer.[34,35] The SH intensities at 420 and 460 nm as a function of the applied potential are displayed in Figure 7. The Galvani potential difference was swept from 0.05 V, where the ZnTPPC coverage is rather low, to -0.35 V and then swept back to the initial potential at a scan rate of 5 mV s^{-1}. The SH signal at 420 nm related to the nonaggregated form of ZnTPPC exhibits a maximum at the formal ion transfer potential, i.e., -0.25 V. The decrease of the SH signal at more negative potentials is associated with desorption and transfer of nonaggregated ZnTPPC as well as by reabsorption of the SH response at 420 nm by the porphyrin transferred into the organic phase. On the other hand, the onset potential of the SH signal at 460 nm occurs at more negative values than at 420 nm, suggesting that the red-shifted species is formed after increasing the interfacial concentration of the porphyrin. Contrary to the behavior observed for the nonaggregated form, the SH signal at 460 nm does not decrease at potentials more negative than the formal transfer potential. This result clearly shows that the porphyrin aggregates are confined to the interfacial boundary and that the corresponding surface excess is also dependent on the Galvani potential difference. These potential dependence of the SH responses are qualitatively consistent with the electrocapillary curve measured for the same concentration of ZnTPPC (cf. Figures 5 and 7).

The various features of the SH spectrum are also strongly dependent on the applied potentials as illustrated in Figure 8. At 0.20 V, the SH spectrum showed a maximum response at 420 nm, which is resonant with the Soret band of the nonaggregated form. Applying more negative potentials, the SH intensity at 420 nm decreases and the signal centered at 460

nm becomes predominant. The shift of the SH maximum from 420 to 460 nm occurs concomitantly with the increase of the surface coverage as revealed by the electrocapillary curves in Figure 5. These results show that the extent of aggregation at the liquid|liquid boundary can be finely controlled by the tuning the Galvani potential difference. Furthermore, the similar spectral features at −0.25 V with respect to those observed at the neat water|DCE interface (Figure 6) suggest that the specific adsorption of ZnTPPC generates a local electric field which further enhance the porphyrin adsorption. This local electric field combined with the enhancement of the $\chi^{(3)}$ component associated with the excitonic levels in the aggregates appears as the most plausible explanation for the intense SH responses. This conclusion is further supported by the fact that the absolute SH signal resonant with the nonaggregated form is significantly smaller than the signal observed for the aggregates.

4. Conclusions

The specific adsorption of ZnTPPC at the water|1,2-dichloroethane interface manifests itself by the generation of intense SH responses as well as by significant changes in the frequency of the characteristic capillary waves. As the Galvani potential difference approaches the formal transfer potential, the surface coverage increases leading to the formation of aggregates at the liquid|liquid boundary. As the extent of the aggregation increases, the overall intensity of the SH responses increases, and the band in resonance with the Soret band exhibits a significant bathochromic shift. These results evidence the enhancement of the nonlinear optical responses because of excitonic transitions associated with the porphyrin aggregates. At potentials more positive than the formal transfer potential, the surface excess of ZnTPPC decreases and the extent of the interfacial aggregation is small. These potential dependences indicate that the surface coverage and the extent of aggregation can reversibly be controlled by tuning the Galvani potential difference.

Acknowledgment. This work was supported by the Fonds National Suisse de la Recherche Scientifique (No. 20-55692.98). H.N. thanks the Grant-in-Aid for Scientific Research of Priority Areas (No. 13129204) from the Ministry of Education, Culture, Sports, Science and Technology of Japan. Z.S. gratefully acknowledges Visiting Fellowship from the EPFL and the financial support from the Grant Agency of the Czech Republic (No. 203/01/0946). The authors also thank Dr. Alastair Wark of the University of Wisconsin, Jean-Pierre Abid, and Dr. Henrik Jensen for valuable discussions.

References and Notes

(1) Falk, J. E. In *Porphyrins and Metalloporphyrins*; Smith, K. M., Eds.; Elsevier: New York, 1975; section B.
(2) Dolphin, D. *The Porphyrins*; Academic Press: New York, 1978.
(3) Kalyanasundaram, K. *Photochemistry of Polypyridine and Porphyrin Complexes*; Academic Press: London, 1992.
(4) Goldberg, I. *Chem. Eur. J.* **2000**, *6*, 3863−3870.
(5) Imamura, T.; Fukushima, K. *Coord. Chem. Rev.* **2000**, *198*, 133−156.
(6) Saitoh, Y.; Watarai, H. *Bull. Chem. Soc. Jpn.* **1997**, *70*, 351−358.
(7) Nagatani, H.; Watarai, H. *Anal. Chem.* **1998**, *70*, 2860−2865.
(8) Duong, H. D.; Brevet, P. F.; Girault, H. H. *J. Photochem. Photobiol. A* **1998**, *117*, 27−33.
(9) Nagatani, H.; Watarai, H. *Chem. Lett.* **1999**, 701−702.
(10) Nagatani, H.; Iglesias, R. A.; Fermín, D. J.; Brevet, P. F.; Girault, H. H. *J. Phys. Chem. B* **2000**, *104*, 6869−6876.
(11) Fermín, D. J.; Ding, Z.; Duong, H.; Brevet, P.-F.; Girault, H. H. *J. Phys. Chem. B.* **1998**, *102*, 10334−10341.
(12) Fermín, D. J.; Duong, H.; Ding, Z.; Brevet, P.-F.; Girault, H. H. *J. Am. Chem. Soc.* **1999**, *121*, 10203−10210.
(13) Jensen, H.; Kakkassery, J. J.; Nagatani, H.; Fermín, D. J.; Girault, H. H. *J. Am. Chem. Soc.*, **2000**, *122*, 10943−10948.
(14) Osakai, T.; Muto, K. *J. Electroanal. Chem.* **2001**, *496*, 95−102.
(15) Fermín, D. J.; Lahtinen, R. In *Liquid interfaces in chemical, biological and pharmaceutical applications*; Volkov, A. G., Eds.; Marcel Dekker Inc.: New York, 2001; pp 179−228.
(16) Fermín, D. J.; Duong, H.; Ding, Z.; Brevet, P.-F.; Girault, H. H. *Phys. Chem. Chem. Phys.* **1999**, *1*, 1461−1467.
(17) Jensen, H.; Fermin, D. J.; Girault, H. H. *Phys. Chem. Chem. Phys.* **2001**, *3*, 2503−2508.
(18) Corn, R. M.; Higgins, D. A. *Chem. Rev.* **1994**, *94*, 107−125.
(19) Eisenthal, K. B. *Chem. Rev.* **1996**, *96*, 1343−1360.
(20) Nagatani, H.; Piron, A.; Brevet, P.-F.; Fermín, D. J.; Girault, H. H. *Langmuir* **2002**, *18*, 6647−6652.
(21) Lofgren, H.; Neuman, R. D.; Scriven, L. E.; Davis, H. T. *J. Colloid Interface Sci.* **1984**, *98*, 175−183.
(22) Jon, D. I.; Rosano, H. L.; Cummins, H. Z. *J. Colloid Interface Sci.* **1986**, *114*, 330−341.
(23) Takahashi, S.; Harata, A.; Kitamori, T.; Sawada, T. *Anal. Sci.* **1994**, *10*, 305−308.
(24) Trojanek, A.; Krtil, P.; Samec, Z. *J. Electroanal. Chem.* **2001**, *517*, 77−84.
(25) Lamb, H. *Hydrodynamics*; Dover: New York, 1945.
(26) Trojanek, A.; Krtil, P.; Samec, Z. *Electrochem. Comm.* **2001**, *3*, 613−618.
(27) Suslick, K. S.; Chen, C. T.; Meredith, G. R.; Cheng, L. T. *J. Am. Chem. Soc.* **1992**, *114*, 6928−6930.
(28) Sen, A.; Ray, P. C.; P. K., D.; Krishnan, V. J. *J. Phys. Chem.* **1996**, *100*, 19611−19613.
(29) Khairutdinov, R. F.; Serpone, N. *J. Phys. Chem. B* **1999**, *103*, 761−769.
(30) Spano, F. C.; Mukamel, S. *Phys. Rev. A* **1989**, *40*, 5783−5801.
(31) Spano, F. C.; Mukamel, S. *Phys. Rev. Lett.* **1991**, *66*, 1197−1200.
(32) Leegwater, J. A.; Mukamel, S. *Phys. Rev. A* **1992**, *46*, 452−464.
(33) Knoester, J. *Adv. Matter.* **1995**, *7*, 500−502.
(34) Nagatani, H.; Fermin, D. J.; Girault, H. H. *J. Phys. Chem. B* **2001**, *105*, 9463−9473.
(35) Kakiuchi, T. *J. Electroanal. Chem.* **2001**, *496*, 137−142.